STRUCTURAL CONTROL AND HEALTH MONITORING
Struct. Control Health Monit. 2008; **15**:416–435
Published online 4 February 2008 in Wiley InterScience
(www.interscience.wiley.com) DOI: 10.1002/stc.245

Identification of the nonlinear behaviour of a cracked RC beam through the statistical analysis of the dynamic response

M. Breccolotti*,†, A. L. Materazzi and I. Venanzi

Department of Civil and Environmental Engineering, University of Perugia, Via G. Duranti, 06125 Perugia, Italy

SUMMARY

This study investigates a new identification procedure suitable to deal with nonlinear systems. The proposed approach is made up of three main parts: system excitation with a band-limited white noise, solution of the Fokker–Planck equation that describes the motion of the structure in a parametric form and identification of the unknown system parameters by minimizing a suitable functional. The new procedure is able, for instance, to assess the severity of cracking caused by the shrinkage or by the overcoming of the concrete tensile strength in reinforced concrete (RC) structures. Cracked RC elements, in fact, exhibit a nonlinear behaviour due to different values of the flexural stiffness that depends on the opening of the cracks. Some numerical simulations allowed verifying the applicability of the procedure. Copyright © 2008 John Wiley & Sons, Ltd.

KEY WORDS: cracked RC element; nonlinear behaviour; identification; Gaussian excitation; Fokker–Planck equation

1. INTRODUCTION

Control and monitoring of existing structures, especially of bridges, is becoming of prime importance in civil engineering. In fact the observation of the bridges belonging to great road and highway networks, such as in the U.S. or in the E.U., shows that many of them are badly damaged. The budget needed for their refurbishment seems to be quite impressive. Hence, a rational plan to proceed to the repairs following a list of precedence is absolutely necessary. Within this framework many studies have been carried out since the 1970s on the application of

*Correspondence to: M. Breccolotti, Department of Civil and Environmental Engineering, University of Perugia, Via G. Duranti 93, 06125 Perugia, Italy.
† E-mail: breccolotti@strutture.unipg.it

Contract/grant sponsor: Italian Ministry for the Education, The University and the Scientific Research (MIUR); contract/grant number: PRIN '04—VinCES (Vibrations in Civil Engineering Structures)

Received 15 February 2007
Revised 5 September 2007
Accepted 16 December 2007

experimental methods, based on dynamic tests, to asses the maintenance condition of the most important infrastructures [1, 2]. The detection of structural damage through dynamic methods is a complex task, as the parameters involved in the process (natural frequencies, modal shapes, damping) depend mainly on the global stiffness and therefore are only slightly influenced by local damages, which, usually, threaten safety. In fact the estimate of the structural safety is made difficult by the weak correlation between the members' stiffness and the mechanical strength of the members' cross sections [3]. Moreover, it must be pointed out that most investigation methods require the preventive knowledge of the dynamic characteristics of the undamaged structure, information that is available only in a few cases. After the first studies, based on the changes of the natural frequencies of vibration [4] and on the damage-induced modification of the modal shapes [5, 6], the present trend is toward the application of advanced techniques to the analysis of the dynamic response, such as statistical methods, proper damage indexes, model updating, neural networks, etc. Modal analysis methods, such as the modal assurance criterion (MAC) and the coordinate modal assurance criterion (COMAC), have been used with success by Fryba and Pirner [7] who compared the dynamic behaviour of two identical bridges, one damaged and the other undamaged, taking the undamaged one as reference. Brincker *et al*. [8] reported their experience in a wide set of progressive damage tests, artificially realized on a bridge in Switzerland that afterwards was razed and replaced by a new one, using a technique called enhanced frequency domain decomposition (FDD), based on the determination of eigenfrequencies, eigenvectors and damping changes. The authors observed that their studies were carried out without taking into account the influence of the temperature and effect that, in their opinion, could prevent the detection of small changes of the modal parameters. Just a few studies concern the assessment of prestressed or reinforced concrete (RC) structures, a task that is much more difficult than evaluating structures made of homogeneous materials. The main reason is that the cracks crossed by the reinforcement, alternatively open and close during the vibration, giving rise to changes in the dynamic response of the structural element. The nonlinearity of damaged RC elements was recently studied jointly in the time–frequency domain by Owen *et al*. [9] and by Neild *et al*. [10]. A finite element model for damaged RC elements based on the theory of fracture mechanics was proposed by Saavedra and Cuitio [11]. Also Petryna and Krtzig [12] proposed a procedure for damage evaluation based on the strip modelling of prestressed or RC structures. All these methods, making use of the natural frequencies and the modal shapes of the investigated system, are affected by the uncertainties due to the environmental factors and require the knowledge of the dynamic characteristics of the undamaged structure. Recent researches proposed the use of innovative techniques based on the probabilistic analysis of the dynamic response of RC structures subjected to Gaussian excitation. These methods are based on the observation that the response of a non-linear system to a Gaussian excitation is non-Gaussian and that the upper statistical moments of the response can be used as a measure of the non-Gaussianity of the response and, therefore, as damage indicators [13, 14]. The higher the non-Gaussianity of the response, the higher the nonlinearity of the structure and, thus, the higher the severity of the damage. In this paper a method that is potentially able to identify the cracking state of an RC beam is proposed. It is based on the dynamic excitation of the beam using a band-limited Gaussian white noise force and on the interpretation of the measured response using a parametric Fokker–Planck equation. Unfortunately closed-form solutions of the Fokker–Planck equation exist only under limiting hypotheses that hardly can be satisfied in the field of bridge monitoring, even if some approximate solutions have been presented [15] and the finite element method has also been

DOI: 10.1002/stc

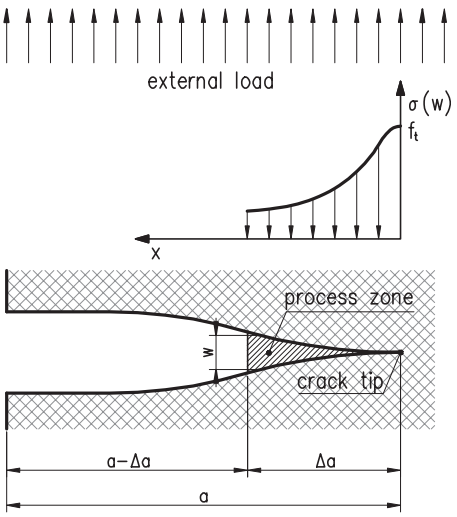

Figure 1. Fracture process zone at the crack tip (adapted from [17]).

used [16]. In the present work the solution is sought using numerical methods by minimizing a suitable functional of the problem parameters.

2. NONLINEAR BEHAVIOUR OF RC BEAMS

The cracking in bending of RC elements submitted to monotonically increasing loads may be studied using the methods of nonlinear fracture mechanics [17]. In the present paper the attention is focused on Mode I fracture, which occurs in case of pure bending. In such a condition, a fracture process zone, whose length is a, develops around the tip of the crack. According to Hilsdorf and Brameshuber [18], the length a may be evaluated in the order of 30–50% of the characteristics length:

$$l_{\mathrm{ch}} = \frac{EG_{\mathrm{F}}}{f_{\mathrm{t}}^2} \tag{1}$$

which depends on the elastic modulus E, the fracture toughness G_{F} and the concrete tensile strength f_{t}. Considering, as an example, a concrete having a characteristic compressive strength $f_{ck} = 42\,\mathrm{N/mm^2}$, a mean tensile strength $f_{\mathrm{t}} = 3.6\,\mathrm{N/mm^2}$, an elastic modulus $E = 35\,000\,\mathrm{N/mm^2}$ and a fracture toughness $G_{\mathrm{F}} = 0.06\,\mathrm{N\,mm/mm^2}$, the value of l_{ch} is 160 mm. Then the length of the process zone is comprised between 48 and 80 mm. The toughness mechanism in the fracture process zone may be modelled, following Hillerborg *et al*. [19], by a cohesive tension $\sigma(w)$, function of the crack tip opening w, acting on the crack surfaces (Figure 1). As a consequence the stress–elongation curve of concrete in tension across the crack assumes the nonlinear shape of Figure 2. Anyway when the behaviour of a cracked RC beam element is considered, the global stiffness only slightly departs from linearity. In fact the bending moment transmitted across the crack tips by means of the cohesive tension $\sigma(w)$ is negligible with respect to that carried by the rebars, because of the moderate value of $\sigma(w)$ and as the process zone,

DOI: 10.1002/stc

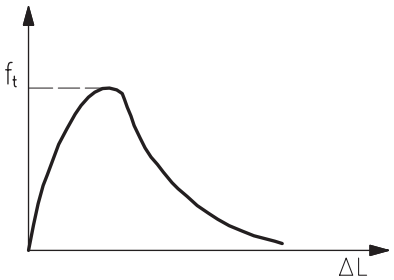

Figure 2. Stress–elongation curve of concrete across a crack.

whose extent is only a small fraction of the crack length, is near to the neutral axis. On the contrary, the rebars carry far greater tensile forces than the concrete in the process zone and are placed in a more favourable position.

The dynamic behaviour of cracked RC beams shows further peculiar aspects. In particular, the following characteristics have been observed by the authors [20]:

(i) RC elements behave roughly linearly under low-intensity dynamic excitation, even if they are damaged and cracked.
(ii) An increase of the structural nonlinearity under increasing external loads can be observed without any change in the actual damage condition.
(iii) Localized damage, such as the partial cut of the rebars or concrete cover removal, does not affect the overall nonlinearity of the element behaviour.
(iv) Under low-severity cracking, the nonlinearity increases with damage. In fact, when the concrete starts to crack, the RC element begins to behave in a nonlinear way. In this phase the cracks are so small that they can be completely closed even by a low-level external excitation. As the severity of the crack pattern increases, a more evident nonlinear behaviour can be observed. This is due to the fact that the difference between the stiffness of the element with closed cracks and that of the element with open cracks increases.
(v) Under high-severity cracking, the nonlinearity decreases for constant level excitation. The wider the cracks, the bigger the external excitation needed to activate the nonlinear behaviour of the RC element caused by the closure of the cracks. Eventually, for very low levels of the external excitation, a linear behaviour of the element characterized by the flexural stiffness of the element with open cracks can be observed.

A piecewise-linear relationship between bending moment and rotation, as the one depicted in Figure 3, can reasonably justify this behaviour. In fact, if the beam is uncracked, its behaviour is linear (solid line) and its response to a white noise excitation is Gaussian. If the beam is cracked, a residual opening of the cracks still remains even at rest (Figure 4). The amount of the opening (ϑ_2) is related to the depth and number of cracks occurring in the element. If the beam is lightly cracked the value of ϑ_2 is small (dashed line), while it is bigger for a strongly cracked beam (dash-dotted line). For the same reasons discussed previously in the case of static loads, the flexural stiffness during the opening of the cracks may be assumed linear too and the curved fillet between the linear branches may be neglected. Anyway the stiffness depends on the status of the cracks: it is higher if the cracks are closed; it is lower if the cracks are open. Hence, if the external

DOI: 10.1002/stc

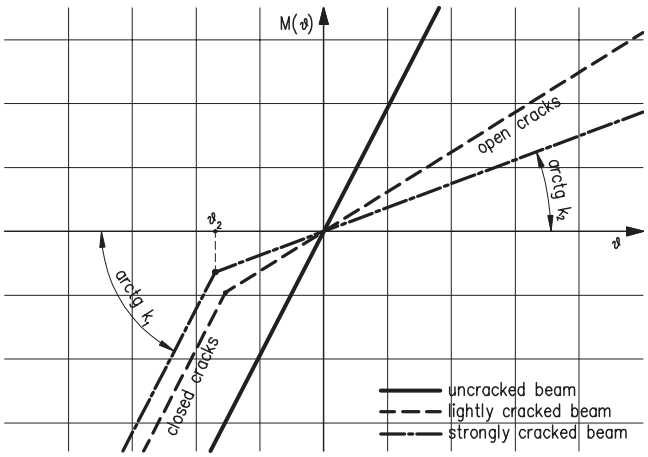

Figure 3. Relationship between bending moment and rotation in a cracked RC element.

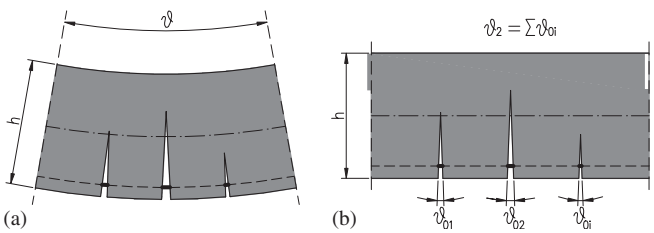

Figure 4. (a) Rotation under loading and (b) residual crack opening at rest of a cracked RC element.

excitation is too low to produce the closure of the cracks, the element behaves linearly. If the level of the external excitation is increased, the cracks can close and the element behaves nonlinearly. If the severity of the cracks expressed by the value of the parameter ϑ_2 increases, a stronger external excitation would be necessary to activate the nonlinear behaviour of the cracked RC element. This behaviour has been also observed by Neild *et al.* [10] through instantaneous frequency measurements during experimental tests on cracked RC beams. Naturally, this behaviour can be observed for both positive and negative bending moments, with suitable modifications to Figure 3. It has also been assumed that the cracks length and geometry do not change during the motion caused by the dynamic tests. This hypothesis can reasonably be accepted if we think that the level of the external excitation used for the dynamic tests is far below the level of the excitation expected during the life of the structure. Thus, no further damage can be caused by the execution of the dynamic tests. An increase of the crack pattern can instead be generated only by a stronger external excitation due, for instance, to bigger live load. In the present study we will assume that the position and the extent of the cracked zone are supposed to be known, while the remaining unknowns, K_2 and ϑ_2 of Figure 3, have to be estimated by means of the proposed methodology. It is worth to note that the parameters K_2 and ϑ_2 are relative to an RC element with finite dimensions that can contain several cracks with different depth and amplitude. The parameter ϑ_2 is in this case equal to the

DOI: 10.1002/stc

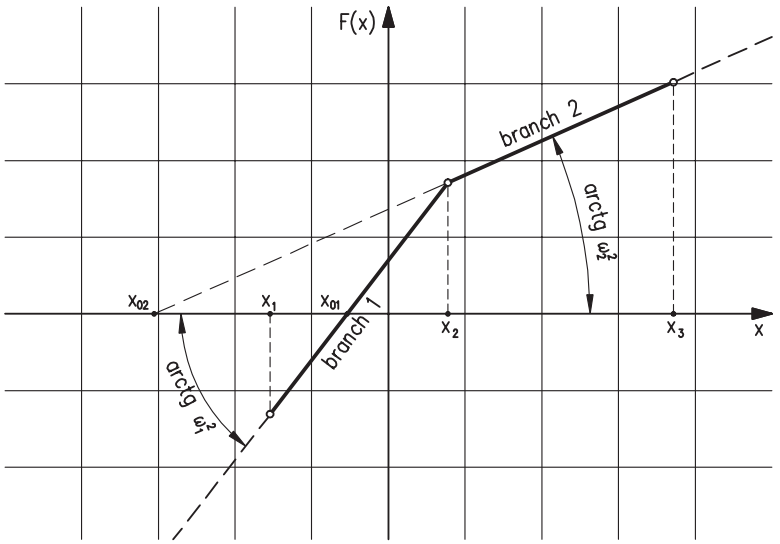

Figure 5. Parameters describing a continuous piecewise-linear restoring force.

sum of the cracks openings at rest $\vartheta_2 = \sum_i \vartheta_{0i}$. No steel rebars yielding is expected since we are dealing with service load conditions.

3. NON-LINEAR IDENTIFICATION

3.1. Theoretical background

The stationary probability density function (PDF) of the response of a single degree of freedom (SDOF) system with continuous piecewise-linear restoring force loaded by a white noise external excitation can be obtained solving the corresponding Fokker–Planck equation. Let the motion of an SDOF system with unit mass be described by the following equation [21]:

$$\ddot{x} + \beta_1 \dot{x} + F_i(x) = f(t) \tag{2}$$

where $F_i(x) = \omega_i^2(x - x_{0i})$ for $x_i \leqslant x \leqslant x_{i+1}, i = 1, 2$ (see Figure 5), ω_i and x_{0i} are suitable constants and $f(t)$ is a weakly homogeneous stochastic process having null mean and spectral density of the form:

$$S_f(\omega) = \frac{S_0}{1 + \omega^2 \tau_0^2} \tag{3}$$

that satisfies the filter equation:

$$\tau_0 \dot{f} + f = \sqrt{S_0}\upsilon(t) \tag{4}$$

DOI: 10.1002/stc

where $v(t)$ is a white noise with unit spectral density, S_0 and τ_0 are positive constants. The corresponding response PDF is

$$w(x,\dot{x}) = \begin{cases} w_1(x,\dot{x}) = C_1 \cdot \mathrm{e}^{-(\omega_1^2/S_0)\beta_1 x^2 + (2x_{01}\omega_1^2/S_0)\beta_1 x} \cdot \mathrm{e}^{-(\beta_1/S_0)\dot{x}^2} = w_{1,x}(x) \cdot w_{\dot{x}}(\dot{x}), & x \leqslant x_2 \\ w_2(x,\dot{x}) = C_2 \cdot \mathrm{e}^{-(\omega_2^2/S_0)\beta_1 x^2} \cdot \mathrm{e}^{-(\beta_1/S_0)\dot{x}^2} = w_{2,x}(x) \cdot w_{\dot{x}}(\dot{x}), & x > x_2 \end{cases} \tag{5}$$

Four additional constraints have to be satisfied:

(1) the continuity condition on the restoring force

$$\omega_2 = \omega_1 \sqrt{\frac{x_2 - x_{01}}{x_2 - x_{02}}} \tag{6}$$

(2) the continuity of the PDF

$$w_{1x}(x_2) = w_{2x}(x_2) \tag{7}$$

(3) the differentiability of the response's PDF that requires the continuity of the PDF's derivative

$$\left.\frac{\mathrm{d}w_{1x}}{\mathrm{d}x}\right|_{x_2} = \left.\frac{\mathrm{d}w_{2x}}{\mathrm{d}x}\right|_{x_2} \tag{8}$$

(4) the normalization condition of the PDF

$$\int_{-\infty}^{+\infty} w_x(x)\,\mathrm{d}x = 1 \tag{9}$$

In the case of SDOF system having mass different from unity, Equation (2) becomes

$$m\ddot{x} + c\dot{x} + R_i(x) = r(t) \tag{10}$$

It can be rewritten as

$$\ddot{x} + \frac{c}{m}\dot{x} + \frac{R_i(x)}{m} = \frac{r(t)}{m} \tag{11}$$

It can be noted that Equations (2) and (11) are identical with the positions: $\beta_1 = c/m$, $F_i(x) = R_i(x)/m$ and $f(t) = r(t)/m$.

3.2. Generalized SDOF system

As mentioned in Section 1, the exact solution of the Fokker–Planck equation for multiple degree of freedom systems exists only in a very few cases. Nevertheless, there is a wide class of structures whose motion can be conveniently approximated by an SDOF system [22]. In these cases, the more the deformed shape of the system can be described by only one deflected shape, the more accurate results can be obtained by the analysis of the corresponding generalized SDOF system. For our purposes, in order to express the equation of the dynamic equilibrium for a continuous beam in the form of a generalized SDOF system:

$$\tilde{m}\ddot{\eta} + \tilde{c}\dot{\eta} + \tilde{k}\eta = \tilde{r}(t) \tag{12}$$

the generalized mass $\tilde{m}$, the generalized damping $\tilde{c}$, the generalized stiffness $\tilde{k}$ and the generalized force $\tilde{r}(t)$ associated with the generalized displacement η must be evaluated. Applying

DOI: 10.1002/stc

the principle of virtual displacement to a beam, it is possible to calculate the following quantities:

$$\tilde{m} = \int_0^L m(x) \cdot \psi^2(x) \cdot \mathrm{d}x \tag{13}$$

$$\tilde{k} = \int_0^L k(x) \cdot \psi''^2(x) \cdot \mathrm{d}x \tag{14}$$

$$\tilde{c} = \int_0^L c(x) \cdot \psi^2(x) \cdot \mathrm{d}x \tag{15}$$

$$\tilde{r}(t) = \int_0^L r(x,t) \cdot \psi(x) \cdot \mathrm{d}x \tag{16}$$

where L is the length of the beam and $\psi(x)$ is the shape function assumed to describe the deflection of the beam. Naturally, the generalized stiffness $\tilde{k}$ has to be calculated taking into account, if necessary, the nonlinear stiffness of the dynamical system. As shape function $\psi(x)$, the static deflection or a modal shape may be alternatively used. If the system is linear the 1st modal shape may be conveniently taken as the shape function. The modal analysis can no longer be applied to nonlinear systems. In the evaluation of the generalized damping $\tilde{c}$ the distributed damping may be taken as

$$c(x) = \frac{2\xi_1 \omega_1 m_1}{L} \tag{17}$$

where ξ_1, ω_1 and m_1 are the relative damping, the natural frequency and the participating mass of the 1st mode evaluated in the case of open cracks. For the evaluation of the Equations (13)–(16), the choice of taking as shape function the static deflection during the fully open crack phase proved by numerical analyses to give more accurate results and for this reason has been used. Let us now consider the non-uniform stiffness, simply supported beam subjected to the concentrated load $F(t)$ at midspan shown in Figure 6. The beam stiffness is EJ_1 near the supports for an extent a by each side and $EJ_2 < EJ_1$ around the midspan for an extent $L - 2a$. The stiffness EJ_2 is representative of the cracked zone.

The relationship between the force $F(t)$ and the displacement η at midspan is

$$\eta\left(\frac{L}{2}\right) = \frac{FL^3}{48EJ_2} + \frac{Fa^3J_2 - J_1}{6 \quad EJ_1J_2} \tag{18}$$

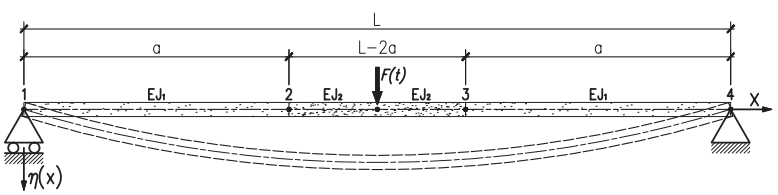

Figure 6. Non-uniform stiffness beam.

DOI: 10.1002/stc

while the general relationship between the force $F(t)$ and the displacement η at a section placed at a distance x from the left support is

$$\eta(x) = \begin{cases} \left(\dfrac{FL^2}{16EJ_2} + \dfrac{Fa^2}{4EJ_1}\dfrac{J_2 - J_1}{J_2}\right)x - \dfrac{Fx^3}{12EJ_1}, & 0 < x < a \\ \dfrac{FL^2 x}{16EJ_2} + \dfrac{Fa^3}{6EJ_1}\dfrac{J_2 - J_1}{J_2} - \dfrac{Fx^3}{12EJ_2}, & a < x < \dfrac{L}{2} \end{cases} \tag{19}$$

If the deflection of the whole beam is expressed in term's of its midspan deflection, the shape function $\psi(x)$ may be expressed as follows:

$$\eta(x) = \eta\left(\frac{L}{2}\right) \cdot \psi(x) \tag{20}$$

Consequently, the deflection η at $x = L/2$ may be assumed as Lagrangian coordinate for the generalized SDOF system. The shape function $\psi(x)$ is thus equal to

$$\psi(x) = \begin{cases} \dfrac{\dfrac{L^2}{16} + \dfrac{a^2}{4}\dfrac{J_2 - J_1}{J_1}}{\dfrac{L^3}{48} + \dfrac{a^3}{6}\dfrac{J_2 - J_1}{J_1}}x - \dfrac{1}{\dfrac{L^3 J_2}{4\,J_1} + 2a^3\dfrac{J_2 - J_1}{J_2}}x^3, & 0 < x < a \\ \dfrac{\dfrac{a^3}{6}\dfrac{J_2 - J_1}{J_1}}{\dfrac{L^3}{48} + \dfrac{a^3}{6}\dfrac{J_2 - J_1}{J_1}} + \dfrac{\dfrac{L^2}{16}}{\dfrac{L^3}{48} + \dfrac{a^3}{6}\dfrac{J_2 - J_1}{J_1}}x - \dfrac{1}{\dfrac{L^3}{4} + 2a^3\dfrac{J_2 - J_1}{J_1}}x^3, & a < x < \dfrac{L}{2} \end{cases} \tag{21}$$

while its second derivative with respect to the x variable is

$$\psi''(x) = \begin{cases} -\dfrac{6}{\dfrac{L^3}{4}\dfrac{J_2}{J_1} + 2a^3\dfrac{J_2 - J_1}{J_2}}x, & 0 < x < a \\ -\dfrac{6}{\dfrac{L^3}{4} + 2a^3\dfrac{J_2 - J_1}{J_1}}x^3, & a < x < \dfrac{L}{2} \end{cases} \tag{22}$$

3.3. Identification of the nonlinear behaviour due to cracking

The identification of the mechanical parameters, i.e. damping and stiffness, in Equation (10) can be achieved by solving an inverse dynamic-stochastic problem. Based on the theoretical background presented in the previous sections, a procedure to identify a structural system excited by Gaussian white noise has been established. The identification can be carried out through the following steps:

(i) System excitation using a band-limited white noise. The system, whose mechanical parameters are unknown, is excited by means of a Gaussian band-limited white noise. An excitation of this type can be generated, for instance, by means of an electrodynamic shaker driven by a closed-loop controller, which generates the excitation according to a prescribed power spectral density value S_0.

DOI: 10.1002/stc

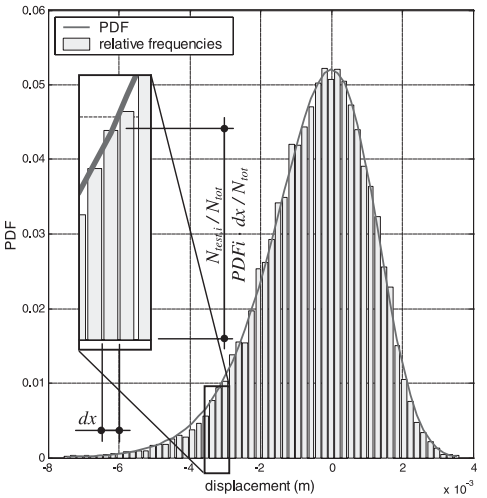

Figure 7. Evaluation of the displacement's relative frequencies from simulated data and tentative PDF.

(ii) Measurement of the response. The procedure requires that the system's response, in terms of displacements and velocities, is known by measurement.

(iii) Evaluation of the structural damping c using the FP equation. Recalling that the velocity's PDF is Gaussian (Equation (5)) with standard deviation equal to

$$\sigma_{\dot{x}} = \sqrt{\frac{S_0}{2cm}} \tag{23}$$

The measurement of the velocity directly allows the determination of the system damping:

$$c = \frac{S_0}{2m\sigma_{\dot{x}}^2} \tag{24}$$

(iv) Evaluation of the parameters that identify the nonlinear restoring force. The parameters $\omega_1, \omega_2, C_1, C_2$ and x_{01} that define the nonlinear behaviour of the system of Figure 5 are identified by minimizing the functional:

$$J = \int_{-\infty}^{+\infty} [w_{\text{test}}(x) - w_x(x)]^2 \, \mathrm{d}x \tag{25}$$

that depends on the PDF of the measured data (w_{test}) and on the response's PDF obtained placing tentative values of the parameters ω_1, ω_2, C_1, C_2 and x_{01} in Equation (5). Since the system response is measured at discrete times, the functional J may be conveniently approximated by means of the finite sum (Figure 7):

$$J = \sum_{i=1}^{n} \left[\frac{N_{\text{test},i}}{N_{\text{tot}}} - \frac{N_{x,i}(x_i)}{N_{\text{tot}}} \right]^2 \tag{26}$$

where N_{tot} is the number of samples and the ratios $N_{\text{test},i}/N_{\text{tot}}$ and $\text{PDF}_i \cdot \mathrm{d}x/N_{\text{tot}}$ are the ith relative frequencies.

DOI: 10.1002/stc

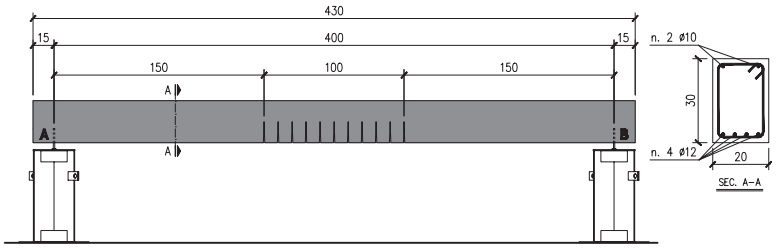

Figure 8. Cracked RC beam considered in the numerical simulations.

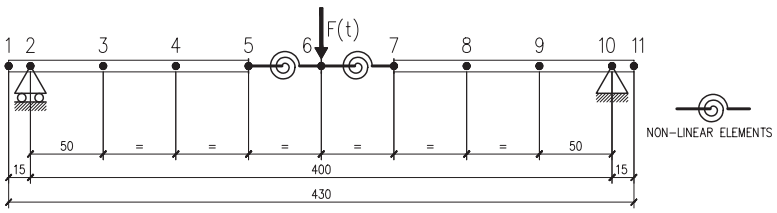

Figure 9. Nonlinear FE model used in the numerical simulations.

A numerical procedure making use of a genetic algorithm (GA) optimization technique has been implemented in a Matlab environment to find the unknown parameters. The GA approach was chosen for its capability to find global minimum rather than local minima in the search space and for its capability of dealing with a high number of unknown parameters to be estimated. The GA, which is based on natural selection, repeatedly modifies a population of individual solutions selecting at random, at each step, individuals from the current population to be parents and using them to produce the children for the next generation. Over successive generations, the population 'evolves' towards an optimal solution. An initial population of 10 000 vectors of the unknown parameters ω_1, ω_2, C_1, C_2 and x_{01} has been used. The cost function implemented in the GA is the functional J reported in Equation (26), subjected to the constraints represented by Equations (6)–(9). These nonlinear constraints have been taken into account using the augmented Lagrangian genetic algorithm by Conn *et al.* [23, 24]. The extension of this procedure to the generalized SDOF is straightforward, taking into account the considerations made in the previous section.

4. NUMERICAL EXAMPLE

4.1. Characteristics of the cracked RC beam used in the simulations

To test the nonlinear identification procedure described in the previous section, a nonlinear FE model representing a cracked RC beam has been defined (Figure 8). It represents a simply supported RC beam, 4.3 m long, made of concrete, having a characteristic compressive strength $f_{ck} = 42\,\mathrm{N/mm^2}$. Its prismatic cross section is 20×30 cm while the clear length between the supports is 4.0 m. The beam is supposed cracked at midspan with an extension of the cracked

DOI: 10.1002/stc

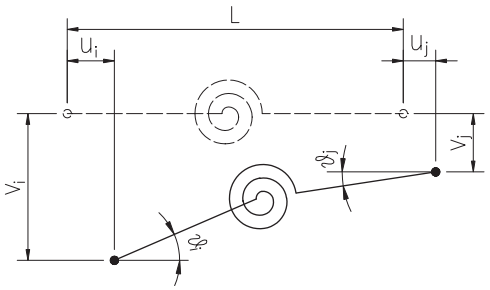

Figure 10. End displacements for the nonlinear element.

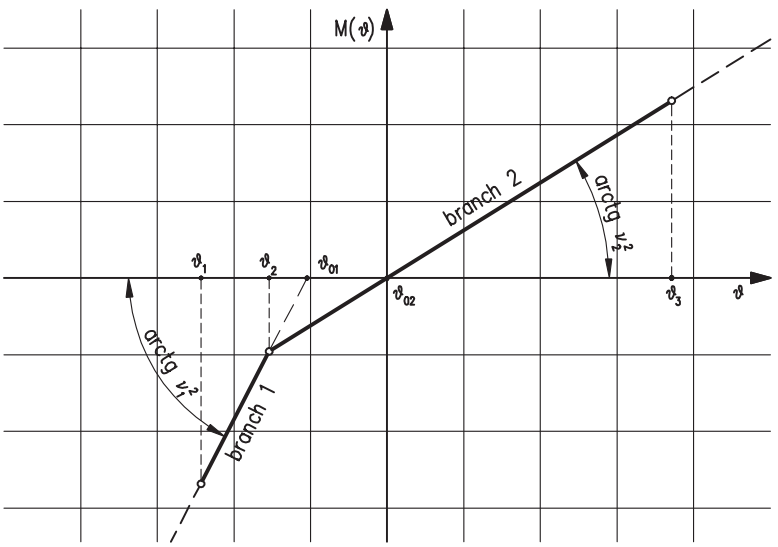

Figure 11. Parameters describing the continuous piecewise-linear restoring moment.

zone of 1.0 m. The reinforcement is made with four 12 mm rebars in tension and two 12 mm rebars in compression. The stirrups, built with 8 mm rebars, are placed every 10 mm.

4.2. FE model

The FE model representing the cracked RC beam is shown in Figure 9. It is made up of eight linear frame elements and two nonlinear frame elements placed in the middle part of the beam. Thus, all the nonlinearities have been concentrated into two nonlinear elements characterized by the following force–displacement relationship:

$$\begin{Bmatrix} P \\ V \\ M \end{Bmatrix} = \begin{bmatrix} k_u & 0 & 0 \\ & k_v & 0 \\ \text{sym.} & & k_\vartheta + L^2/4 \cdot k_v \end{bmatrix} \cdot \begin{Bmatrix} u \\ v \\ \vartheta \end{Bmatrix} \tag{27}$$

DOI: 10.1002/stc

where P, V and M are, respectively, the internal axial force, the shear force and the bending moment; k_u and k_v are the axial and transversal linear stiffness; u, v and ϑ are the relative axial displacement, the relative transversal displacement and the relative rotation between the end sections of the element (Figure 10), defined as

$$\begin{aligned} u &= u_i - u_j \\ v &= v_i - v_j \\ \vartheta &= \vartheta_i - \vartheta_j \end{aligned} \tag{28}$$

The moment–rotation relationship k_ϑ is nonlinear. It is described by the equation (Figure 11):

$$M = \begin{cases} K_2 \cdot \vartheta & \text{for } \vartheta \geqslant \vartheta_2 \\ K_1 \cdot \vartheta + (K_1 - K_2) \cdot \vartheta_2 & \text{for } \vartheta \leqslant \vartheta_2 \end{cases} \tag{29}$$

The cracks are supposed to be initially open and the flexural stiffness is K_2. Positive rotations further open the cracks, while negative rotations close them. Until the relative rotation ϑ between the ends of the nonlinear element reaches the limiting value ϑ_2 the cracks remain open and the bending stiffness is equal to K_2. For $\vartheta < \vartheta_2$ the cracks are completely closed and the element behaves as an uncracked element with tangent stiffness K_1, greater than K_2. Under low-level external excitation, the relative rotation between the initial and the final section of the cracked element remains in the range $0 < \vartheta < |\vartheta_2|$; thus the response is linear and the system containing the nonlinear elements provides a Gaussian response to a Gaussian excitation. Conversely, under bigger enough external forces, the rotation becomes smaller than ϑ_2, the cracks alternatively open and close, the behaviour becomes nonlinear and the response non-Gaussian.

The increase of the nonlinearity at the first stage of cracking and its decrease for a more developed cracking pattern, as already mentioned in Section 2, can be described by a proper variation of the mechanical parameters K_2 and ϑ_2, while K_1 is assumed to be constant. In the most general damage identification problem the following parameters have to be identified: the number of cracked beam regions, their position and extent, the flexural stiffness of the cracked elements K_2 and the relative rotation causing the complete closure of the cracks ϑ_2. The value of the flexural stiffness of the uncracked region K_1 can be assumed as known.

4.3. Parameters describing the nonlinear behaviour

The bending stiffness K_1 has been calculated taking into account the elastic properties of the uncracked section. The stiffness K_2 has been calculated neglecting the contribution of concrete in tension, applying the hypotheses commonly used in the strength analysis of RC sections. Assuming that the curvature remains constant along the nonlinear spring elements, the parameters K_1 and K_2 are

$$\begin{aligned} K_1 &= \frac{E \cdot J_1}{l} = \frac{4.03\text{e}7\,\text{kN/m}^2 \cdot 0.000492\,\text{m}^4}{0.50\,\text{m}} = 39623.6\,\text{kNm} \\ K_2 &= \frac{E \cdot J_2}{l} = \frac{4.03\text{e}7\,\text{kN/m}^2 \cdot 0.000128\,\text{m}^4}{0.50\,\text{m}} = 10299.9\,\text{kNm} \end{aligned} \tag{30}$$

where E is the concrete elastic modulus, l is the length of the element and J_1 and J_2 are the moments of inertia of the uncracked and cracked section, respectively. The beam has a mass per

DOI: 10.1002/stc

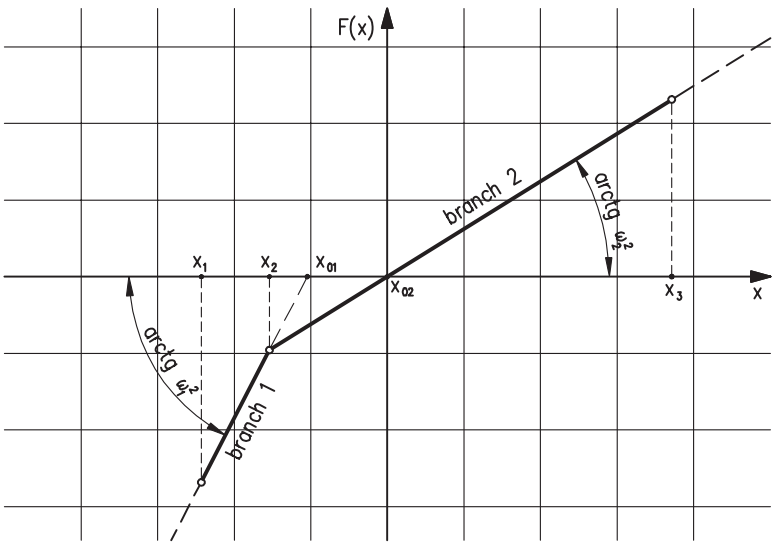

Figure 12. Parameters describing a continuous piecewise-linear restoring force.

unit length equal to 0.144 t/m. Recalling Equation (13) and using the shape function of Equation (21), the mass $\tilde{m}$ of the generalized SDOF system has been calculated. Similarly, integrating the Equation (15), the corresponding value of the damping $\tilde{c}$ has been obtained. Their values are $\tilde{m} = 0.254$ t, $\tilde{c} = 0.934\,\mathrm{kN\,s\,m^{-1}}$. The generalized force $\tilde{r}(t)$ associated with the assumed shape function is equal to the external excitation acting at the midspan of the beam. In fact,

$$\tilde{r}(t) = \int_0^L r(x,t)\cdot\psi(x)\cdot\,\mathrm{d}x = \int_0^L r(t)\cdot\delta\left(x-\frac{L}{2}\right)\cdot\psi(x)\cdot\,\mathrm{d}x = r(t)\cdot\psi\left(\frac{L}{2}\right) = r(t) \qquad (31)$$

where δ is the Dirac delta function and $\psi(L/2) = 1$ from Equation (21). To reduce the nonlinear beam to a nonlinear SDOF system it is necessary to define its nonlinear restoring law. Referring to Figure 6, for positive displacement ($\eta > 0$) the cracks shown in the Figure 8 further open and the behaviour is linear. For negative displacements the behaviour of the beam remains linear until the cracks are completely closed. This happens when the value of the bending moment in the nonlinear element verifies the following equality:

$$\vartheta(M) = \int_0^L \frac{M}{EJ_2}\cdot\,\mathrm{d}x = \vartheta_2 \qquad (32)$$

where ϑ_2 represents the total value of the crack openings of the beam at rest (Figure 4). Considering the values of flexural stiffness reported in Equation (28) the nonlinear relation between rotation and moment at the beam's midspan is shown in Figure 11, where the parameters assume the values: $\upsilon_1 = 199.05\,\mathrm{kN^{0.5}\,m^{0.5}\,rad^{-0.5}}$, $\upsilon_2 = 101.49\,\mathrm{kN^{0.5}\,m^{0.5}\,rad^{-0.5}}$, $\vartheta_2 = -4.85\times10^{-4}$ rad, $\vartheta_{01} = -3.59\times10^{-4}$ rad, $\vartheta_{02} = 0.00$ rad.

The corresponding relation between the displacement and the external force at midspan is represented in Figure 12 where the parameters that define this relationship are $\omega_1 = 121.9\ \mathrm{kN^{0.5}\,m^{-0.5}}$, $\omega_2 = 74.9\,\mathrm{kN^{0.5}\,m^{-0.5}}$, $x_2 = -0.89$ mm, $m_1 = -0.55$ mm, $m_2 = 0.00$ mm.

DOI: 10.1002/stc

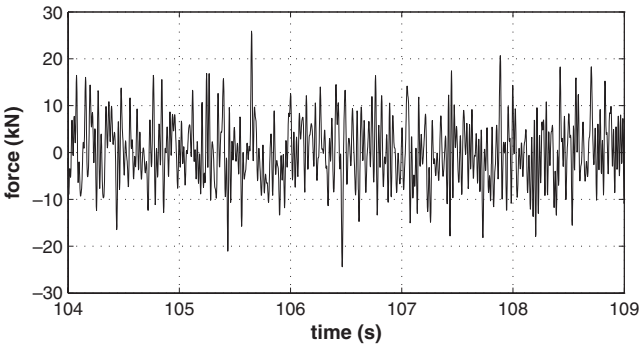

Figure 13. Sample of the time history of the forcing function used in the simulation.

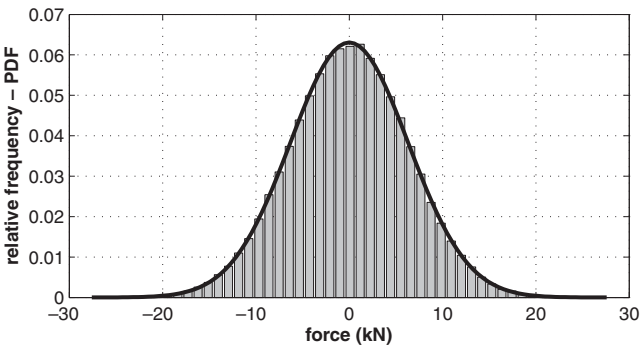

Figure 14. PDF of the forcing function.

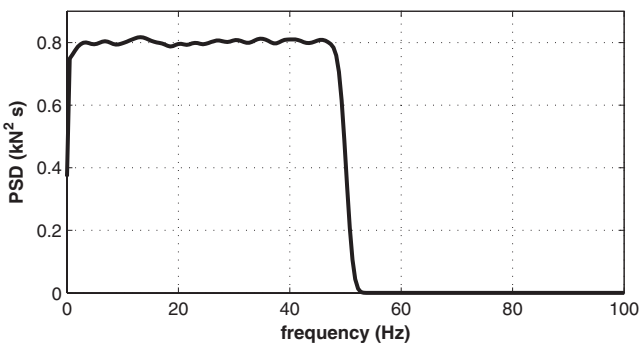

Figure 15. PSD of the forcing function.

4.4. External excitation

An artificial white noise external force has been applied at the midspan of the beam (node no. 6 in the FE model). This force simulates the one that could be generated during an experimental test through a closed-loop control electrodynamic shaker. The artificial external force has been

DOI: 10.1002/stc

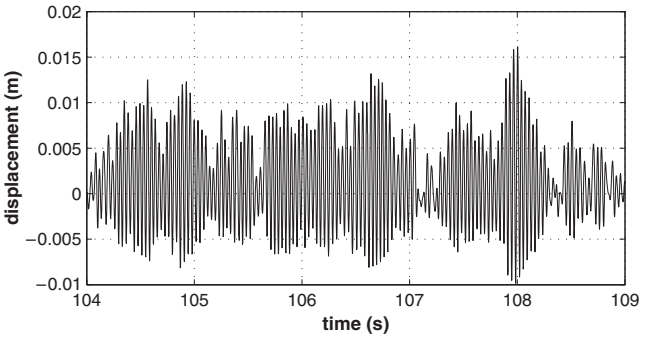

Figure 16. Sample of the time histories of the displacement.

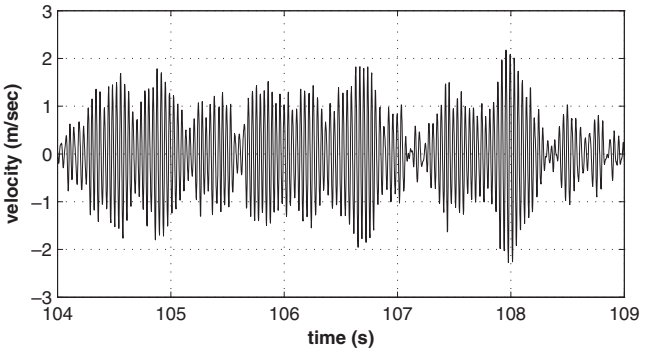

Figure 17. Sample of the time histories of the velocity.

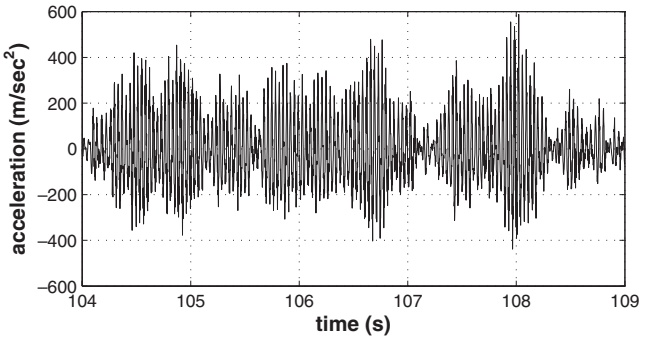

Figure 18. Sample of the time histories of the acceleration.

generated to be compatible with a constant power spectral density of $0.8\,\mathrm{kN^2\,s}$ in the range 0.10–50.1 Hz, applying the well-known algorithm proposed by Shinozuka and Jan [25]. The duration of the excitation has been set to 300 s with a sampling frequency of 500 Hz. The time history of the force, its PDF and its power spectral density (PSD) are depicted in Figures 13, 14 and 15, respectively.

DOI: 10.1002/stc

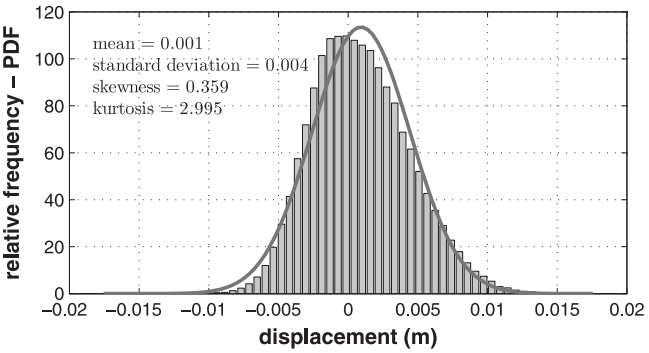

Figure 19. Relative frequencies of the displacement.

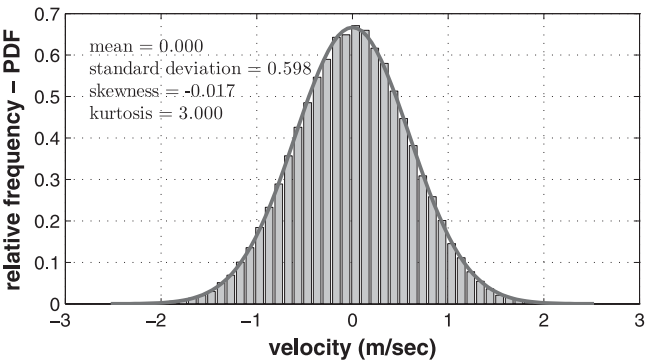

Figure 20. Relative frequencies of the velocity.

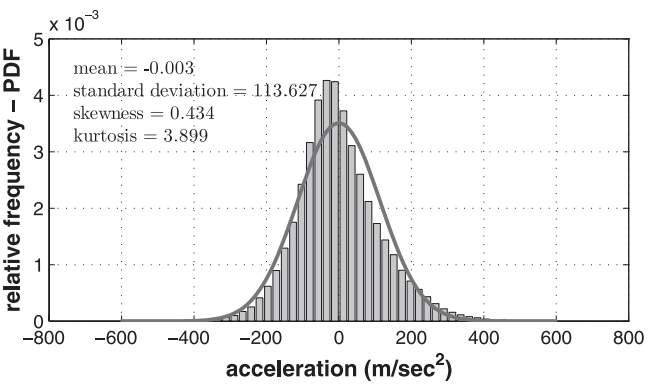

Figure 21. Relative frequencies of the acceleration.

4.5. Results of the numerical simulations

The displacement, the velocity and the acceleration time histories of the node at midspan have been numerically evaluated by direct integration of the equations of motion, using the HHT algorithm [26]. Samples of the time histories of displacement, velocity and acceleration are shown in the Figures 16–18. In Figures 19–21 are given the distributions of the relative

DOI: 10.1002/stc

Table I. Comparison between actual and identified parameters.

	Actual value	Identified value	Relative error (%)
c	$0.934\,\mathrm{kN\,s\,m^{-1}}$	$2.005\,\mathrm{kN\,s\,m^{-1}}$	114.7
ω_1	$121.2\,\mathrm{kN^{0.5}\,m^{-0.5}}$	$114.4\,\mathrm{kN^{0.5}\,m^{-0.5}}$	−5.6
x_2	0.89 mm	0.93 mm	4.5
m_1	0.55 mm	0.55 mm	0.0

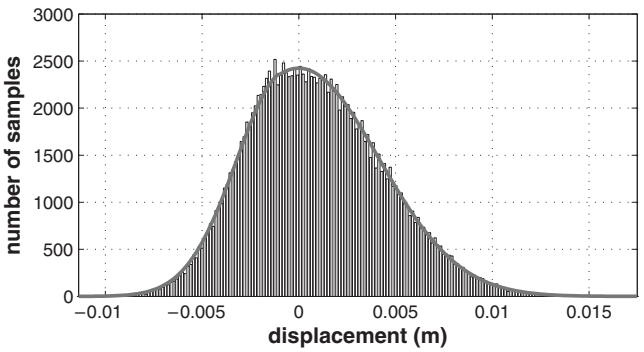

Figure 22. Comparison between numerical simulation and fitted PDF.

frequencies of the displacement, the velocity and the acceleration, respectively, along with the values of the skewness and of the kurtosis that are indicators of the non-Gaussianity of the distributions. On the same figures the PDF of the Gaussian distributions having the same mean and standard deviation are superimposed. It can be noted that the velocity relative to frequencies displays an almost null skewness and a kurtosis equal to 3.00; thus the velocity is Gaussian. In fact the distribution is well approximated by a Gaussian PDF with the same mean value and standard deviation, as foreseen by Lin *et al.* [27, 28]. On the contrary, the displacement and acceleration relative frequencies are quite far from being approximated by normal distributions and their non-Gaussian nature becomes more and more evident as the level of the external excitation increases, in good agreement with the experimental behaviour described in [20].

4.6. Results of the identification procedure

In Table I the results of the identification procedure are summed up, compared with the value used in the FE model to generate the pseudo-experimental data. The damping c of the system has been identified using Equation (24) from the simulated velocity data. The model updating technique and the minimization of the functional J described in Equation (26) allowed the evaluation of the unknown parameters ω_1, x_2 and m_1 with identified values very close to the actual ones.

The displacement PDF corresponding to the identified parameters is depicted in Figure 22 together with the relative frequencies of the displacement data obtained by the numerical simulation. Some comments must be made about the identified value of the damping which is affected by a non-negligible error. In the procedure described in Section 3.2 two simplifying

DOI: 10.1002/stc

hypotheses have been introduced: the determination of the damping of the generalized SDOF system is carried out neglecting the contribution of the higher modes damping and the damping is supposed to be the same for both cracked and uncracked elements. Nevertheless, only in a very few cases the damping represents an important parameter to be identified. Moreover, in the identification procedure described in this paper, the error introduced in the stiffness identification, which is the main object of the overall identification procedure, by a poor estimation of the damping c is quite small, as demonstrated by the numerical results.

5. CONCLUDING REMARKS

Cracked concrete beams exhibit a nonlinear behaviour that depends on the severity of cracking and on the level of the external excitation. It has been observed that the nonlinearity tends initially to increase as the crack pattern gets more severe whereas it tends to decrease as the cracks further widen and deepen and can no longer close under dynamic excitation. The nonlinearity increases, also, with the level of the external excitation. Since the state of cracking can be considered as damage for RC elements, affecting their strength and stiffness at the service limit state, its evaluation is of primary importance. In this paper a new procedure to identify the nonlinear features of cracked RC beams is presented. The method is based on the statistical analysis of the system response when it is subjected to a band-limited white noise, on the theory of Markov process and on the Fokker–Planck equation. The minimization of a suitable functional, which depends on the statistical properties of the responses of the real system and of a parametric numerical model that simulates the *breathing* of the cracked RC beam during the dynamic response, allows the evaluation of the mechanical properties of cracked RC beams. The assessment of the severity of the cracking is hence possible. Several simulations carried out using a numerical model representative of experimental tests allowed to validate the procedure. The obtained results confirmed the applicability of the proposed method.

ACKNOWLEDGEMENTS

The financial support of the Italian Ministry for the Education, the University and the Scientific Research (MIUR) through the PRIN '04—*VinCES* (Vibrations in Civil Engineering Structures) is gratefully acknowledged.

REFERENCES

1. Doebling SW, Farrar CR, Prime MB, Shevitz DW. Damage identification and health monitoring of structural and mechanical system from changes in their vibrational characteristic: a literature review. *Report LA-13070-MS*, Los Alamos National Laboratories, Los Alamos, New Mexico, 1996.
2. Hoon S, Farrar CR, Hemez FM, Czarnecki JJ, Shunk DD, Stinemates DW, Nadler BR. A review of structural health monitoring literature: 1996–2001. *Report LA-13976-MS*, Los Alamos National Laboratories, Los Alamos, New Mexico, 2003.
3. Breccolotti M, Materazzi AL. Reliability of the dynamic methods for evaluating structural concrete bridge integrity. In *Proceedings of the 2nd International Conference on bridge maintenance, safety and management*, Balkema, Leiden, 2004.
4. Lifshitz LM, Rotem A. Determination of reinforcement unbonding of composites by vibration techniques. *Journal of Composites Materials* 1969; **3**(3):412–423.

DOI: 10.1002/stc

5. Salawu OS, Williams C. Damage location using vibration mode shapes. In *Proceedings of IMAC*, Honolulu, U.S.A. 1994; 933–939.
6. Farrar CR, Doebling SW. Lessons learned from application of vibration-based damage identification methods to large bridge structures. In *Proceedings of International Workshop on Structural Health Monitoring*, Stanford CA, 1997; 351–370.
7. Fryba L, Pirner M. Load test and modal analysis of bridges. *Engineering Structures* 2001; **23**(1):102–109.
8. Brincker R, Andersen P, Cantieni R. Identification and level I damage detection of the Z24 highway bridges. *Experimental Techniques* 2001; **25**(6):51–57.
9. Owen JS, Eccles BJ, Choo BS, Woodings MA. The application of auto-regressive time series modelling for the time–frequency analysis of civil engineering structures. *Engineering Structures* 2001; **23**(5):521–536.
10. Neild SA, Williams MS, McFadden PD. Nonlinear vibration characteristic of damaged concrete beams. *Journal of Structural Engineering* 2001; **129**(260):260–268.
11. Saavedra PN, Cuitiño LA. Crack detection and vibration behaviour of cracked beams. *Computers and Structures* 2001; **79**(16):1451–1459.
12. Petryna YS, Krätzig WB. Compliance-based structural damage measure and its sensitivity to uncertainties. *Computers and Structures* 2005; **83**(14):1113–1133.
13. Cacciola P, Muscolino G. Dynamic response of a rectangular beam with a known non-propagating crack of certain or uncertain depth. *Computers and Structures* 2002; **80**(27–30):2387–2396.
14. Cacciola P, Impollonia N, Muscolino G. Crack detection and location in a damaged beam vibrating under white noise. *Computers and Structures* 2003; **81**(18–19):1773–1782.
15. Mosbah H, Fogli M. An original approximate method for estimating the invariant probability distribution of a large class of multi-dimensional nonlinear stochastic oscillators. *Probabilistic Engineering Mechanics* 2003; **18**(2):165–170.
16. Masud A, Bergman LA. Application of multiscale finite element methods to the solution of the Fokker–Planck equation. *Computer Methods in Applied Mechanics and Engineering* 2005; **194**(12–16):1513–1526.
17. Shah SP, Swartz SE, Ouyang C. *Fracture Mechanics of Concrete: Applications of Fracture Mechanics to Concrete, Rock, and Other Quasi-brittle Materials* Wiley: New York, 1995.
18. Hilsdorf HK, Brameshuber W. Code-type formulation of fracture mechanics concepts for concrete. *International Journal of Fracture* 1991; **51**(1):61–72.
19. Hillerborg A, Modeer M, Petersson PE. Analysis of crack formation and crack growth in concrete by means of fracture mechanics and finite elements. *Cement and Concrete Research* 1976; **6**(6):773–782.
20. Breccolotti M, Materazzi AL. RC beams damage detection through probabilistic analysis of the dynamic response. In *Proceedings of 9th International Conference on Structural Safety and Reliability*, Rome, 2005.
21. Piszczec K, Niziol J. *Random Vibration of Mechanical System*. Ellis Horwood: Chichester, 1986.
22. Chopra AK. *Dynamics of Structures*. Prentice-Hall: Englewood Cliffs, NJ, 1995.
23. Conn AR, Gould NIM, Toint PhL. A globally convergent augmented Lagrangian algorithm for optimization with general constraints and simple bounds. *SIAM Journal on Numerical Analysis* 1991; **28**(2):545–572.
24. Conn AR, Gould NIM, Toint PhL. A globally convergent augmented Lagrangian barrier algorithm for optimization with general inequality constraints and simple bounds. *Mathematics of Computation* 1997; **66**(217): 261–288.
25. Shinozuka M, Jan CM. Digital simulation of random processes and its application. *Journal of Sound and Vibration* 1972; **25**:111–128.
26. Hughes TJR. *The Finite Element Method*. Prentice-Hall: Englewood Cliffs, NJ, 1987.
27. Lin YK. *Probabilistic Theory of Structural Dynamics*. McGraw-Hill: New York, 1967.
28. Lin YK, Cai GQ. *Probabilistic Structural Dynamics*. McGraw-Hill: New York, 1995.

DOI: 10.1002/stc